https://doi.org/10.5194/cp-2022-38
Preprint. Discussion started: 9 May 2022
© Author(s) 2022. CC BY 4.0 License.

Climate of the Past Discussions

Is it possible to estimate aerosol optical depth from historic colour paintings?

Christian von Savigny[1], Anna Lange[1], Anne Hemkendreis[2], Christoph G. Hoffmann[1], and Alexei Rozanov[3]

[1]Institute of Physics, University of Greifswald, Felix-Hausdorff-Str. 6, 17489 Greifswald, Germany
[2]Institute of Art History, Albert-Ludwigs-University of Freiburg, Platz der Universität 3, 79085 Freiburg, Germany
[3]Institute of Environmental Physics, University of Bremen, Otto-Hahn-Allee 1, 28359 Bremen, Germany

Correspondence: Christian von Savigny (csavigny@physik.uni-greifswald.de)

Abstract.

The idea of estimating stratospheric aerosol optical thickness from the twilight colours in historic paintings – particularly under conditions of volcanically enhanced stratospheric aerosol loading – is very tantalising, because it would provide information on the stratospheric aerosol loading over a period of several centuries. This idea has in fact been applied in a few studies in order to provide quantitative estimates of the aerosol optical depth after some of the major volcanic eruptions that occurred during the past 500 years. In this study we critically review this approach and come to the conclusion that the uncertainties of the estimated aerosol optical depths are so large that the values have to be considered highly questionable. We show that several auxiliary parameters – which are typically poorly known for historic eruptions – can have a similar effect on the red-green colour ratio as a change in optical depth typically associated with eruptions such as, e.g. Tambora in 1815 or Krakatao in 1883. Among the effects considered here, uncertainties in the aerosol particle size distribution have the largest impact on the colour ratios and hence the aerosol optical depth estimate. For solar zenith angles exceeding 80°, uncertainties in the stratospheric ozone amount can also have a significant impact on the colour ratios. In addition, for solar zenith angles exceeding 90° the colour ratios exhibit a dramatic dependence on solar zenith angle, rendering the estimation of aerosol optical depth essentially impossible.

1 Introduction

Volcanic eruptions constitute one of the largest uncertainty for natural climate variability on time scales of a few years up to a decade (e.g. Robock, 2000; von Savigny et al., 2020). Prominent examples of volcanic eruptions with significant climatic effects are the 1815 eruption of Tambora, which led to the year without summer in 1816 (Raible et al., 2016), or the 1991 eruption of Mt. Pinatubo. Volcanic eruptions provide an important opportunity to improve the scientific understanding of the climate system's response to perturbations. Several sources of information are available for investigating past volcanic activity, e.g. ice cores (e.g. Zielinski et al., 1994), tree-rings (e.g. Esper et al., 2017) or historic reports (e.g. Bauch, 2017). Volcanic eruptions can also lead to significant changes in the colour of the sky, as well as to unusual optical phenomena such as blue or green suns (e.g. Symons et al., 1888; Horvath et al., 1994; Wullenweber et al., 2021) and Bishop's rings (Symons et al.,

https://doi.org/10.5194/cp-2022-38
Preprint. Discussion started: 9 May 2022
© Author(s) 2022. CC BY 4.0 License.

Climate of the Past Discussions

1888). For detailed accounts of unusual optical phenomena associated with volcanic eruptions we refer to the classical works by Kiessling (1888) and Symons et al. (1888). Some studies employed the sky colours in historic paintings to detect evidence for volcanic eruptions and to infer quantitative information on the aerosol optical depth at the time, when the painting was painted (e.g. Zerefos et al., 2007, 2014). The basic idea is to extract the red-green colour ratios of selected areas of the evening sky in photographs of historic paintings and relate these ratios to ratios simulated with a radiative transfer model in order to derive quantitative information on the aerosol optical depth.

In the present study we scrutinise the robustness of the very interesting approach of aerosol optical depth estimations based on colour ratios extracted from photographs of historical paintings and investigate the effect of several additional parameters or processes that also affect the colour ratios, but that were not considered properly in earlier studies. Our initial motivation was to support the approach by providing a better theoretical foundation.

The paper is structured as follows. In section 2 we introduce the radiative transfer model SCIATRAN used in this study to simulate colour ratios. In addition, we briefly introduce the concept of the CIE (International Commission on Illumination) XYZ-tristimulus values that allows for a more realistic simulation of colours perceived by humans than the use of two discrete wavelengths. Section 3 presents simulation results on the dependence of colour ratios and X/Y tristimulus value ratios on several relevant parameters, e.g. the particle size distribution (PSD) of the volcanic aerosol layer, the amount of stratospheric ozone or surface albedo. Section 3 also compares our results to previous studies on this topic. A general discussion of the results is provided in section 4 and conclusions are given at the end.

2 Methodology

We first describe the Mie simulations and the radiative transfer model employed, followed by a summary of the colour modelling approach used in this study.

2.1 Radiative transfer simulation: Mie scattering calculations and SCIATRAN

The radiative transfer simulations presented in this work were carried out with version 4.1.3 of the SCIATRAN radiative transfer model (Rozanov et al., 2014). SCIATRAN is a highly versatile model initially developed for the analysis of remote sensing measurements in the optical spectral range. In the present work, SCIATRAN was run in the approximate spherical mode, where the contribution of single scattering is calculated in a fully spherical geometry, while an approximation is employed to account for the multiple scattering contribution (Rozanov et al., 2000). As discussed by Lange et al. (2022) this approximation is fully sufficient to analyze the colors of the horizon area during twilight. Both the sun-ward near-horizon radiances and the diffuse downward fluxes as analyzed by Zerefos et al. (2007) were modeled with SCIATRAN. The SCIATRAN input parameters relevant to this study are given in Table 1. The volcanic stratospheric aerosol layer considered here has a Gaussian shape of the particle number density profile with a peak altitude of $z_{peak} = 20$ km and a FWHM (Full Width at Half Maximum) of 3 km. The peak altitude and the FWHM were also varied, causing only minor effects on the results. For this reason, only results for $z_{peak} = 20$ km and FWHM = 3 km are presented in this study. The troposphere was assumed to be free of aerosols. More

https://doi.org/10.5194/cp-2022-38
Preprint. Discussion started: 9 May 2022
© Author(s) 2022. CC BY 4.0 License.

Climate of the Past Discussions

Parameter	Abbreviation	Baseline value	Perturbed values
Viewing zenith angle	VZA	85°	70°, 75°, 80°, 90°
Solar azimuth angle*	SAA	10°	20°, 30°, 40°
Stratospheric aerosol optical depth	AOD	N/A	0.0, 0.05, 0.1, 0.2, 0.3
Median radius†	r_{med}	250 nm	150 nm, 350 nm, 450 nm
Geometric width†	S	1.5	N/A
Total ozone column	TOC	300 DU	200 DU, 400 DU
Surface albedo	A_s	0.3	0.1, 0.5, 0.7, 0.9

Table 1. Compilation of the relevant input parameters for the SCIATRAN simulations. Note that the solar zenith angle (SZA) is varied for all case studies in the range from 40° – 96° (* the solar azimuth angle corresponds to the azimuthal angular difference between the viewing direction and position of the sun for a ground-based observer; † parameters of a mono-modal log-normal particle size distribution (see Eqn. 1)).

detailed information on the SCIATRAN radiative transfer model is available in Rozanov et al. (2014) and the SCIATRAN User's Guide (IUP, 2021).

We assume the volcanic aerosol layer to consist of sulfate particles and the refractive index was chosen correspondingly, i.e. $n_r = 1.43 - 1 \times 10^{-8} i$ at a wavelength of 550 nm. Further, we assume a mono-modal log-normal particle size distribution:

$$n(r,z) = \frac{N_0(z)}{\sqrt{2\pi} \cdot \ln(S) \cdot r} \cdot exp\left[-\frac{(\ln r - \ln r_m)^2}{2\ln^2(S)}\right] \quad (1)$$

with N_0 being the particle number density, r_m the median radius, r the particle radius and S the geometric standard deviation of the distribution. Mie scattering phase functions and scattering cross-sections are determined with the Mie scattering routines included in the SCIATRAN radiative transfer model. The simulated spectra were multiplied with a solar irradiation spectrum based on SORCE measurements (LASP, 2003). In addition, we used standard pressure and temperature as well as atmospheric trace gas profiles for tropical latitudes and the month of June taken from a climatological database based on simulations with the 3-D chemical transport model by Sinnhuber et al. (2003).

Using the SCIATRAN calculations of near-horizon radiance or diffuse downward flux spectra covering the 300 nm to 800 nm spectral range, we determine colour ratios based on (a) discrete wavelengths and (b) ratios of the CIE X and Y tristimulus values – which consider certain wavelength ranges in contrast to the discrete wavelengths in (a) – as described below. The tristimulus values are determined by weighting the simulated spectra with the $\overline{x}(\lambda)$ and $\overline{y}(\lambda)$ CIE (International Commission on Illumination) colour matching functions, as described in more detail in, e.g. Wullenweber et al. (2021). The CIE colour matching functions represent the spectral sensitivity functions of the three types of cone cells responsible for human colour vision.

https://doi.org/10.5194/cp-2022-38
Preprint. Discussion started: 9 May 2022
© Author(s) 2022. CC BY 4.0 License.

Climate of the Past Discussions

3 Results

We start in section 3.1 with a brief discussion of the wavelengths used to form the colour ratios based on radiative transfer simulations. In the following sections 3.2 to 3.7 we discuss the effects of different parameters and processes on colour ratios of the evening sky that challenge the estimation of aerosol optical depth from colour ratios extracted from historic paintings.

3.1 Choice of wavelengths for colour ratio simulations

Zerefos et al. (2007) performed radiative transfer simulations and determined the colour ratio using the wavelengths of 700 nm and 550 nm. One issue is that they did not calculate the radiance ratio for a near-horizon viewing geometry, but calculated the ratio of the diffuse downward fluxes at the two wavelengths, although the near-horizon radiance would be the correct quantity in this context. Colour ratios of near-horizon radiances and diffuse downward fluxes show quite a different dependence on AOD, as will be shown in section 3.7 below. Radiance corresponds to the number of photons per unit area, per unit time and per unit solid angle for a given direction, whereas the diffuse downward flux corresponds to the radiance integral over all directions of the upper half sphere, weighted by the cosine of the incidence angle, which gives more weight to smaller incidence angles and almost eliminates contributions from incidence angles close to 90°, corresponding to directions near the horizon. In the current section we focus on the choice of wavelengths. While 550 nm coincides well with the maximum of the $\overline{y}_\lambda$ CIE colour matching function – corresponding to the green-sensitive cones – 700 nm is quite far off the maximum of the $\overline{x}_\lambda$ colour matching function, representing the red-sensitive cones. The maximum of $\overline{x}_\lambda$ is at about 600 nm. For this reason, 700 nm appears to be an unsuitable choice in order to relate modelled colour ratios to red-green colour ratios extracted from pictures of paintings. In addition, at wavelengths of around 700 nm the spectra are affected by an H_2O absorption band that can have a significant impact on the radiance values (see Fig. 1). For this reason, we perform our first tests with a wavelength of 670 nm – rather than 700 nm – which is relatively free of absorption (Fig. 1). Note that we employ 670 nm in order to use a wavelength as close as possible to the wavelength used in Zerefos et al. (2007), but to avoid the H_2O absorption band near 700 nm.

In the following, we will also determine colour ratios based on the X and Y tristimulus values, which better represent the colour sensitivity of the human eye's cone cells. The red-green colour ratio is then represented by the ratio X/Y. Note that the scattering spectra simulated with SCIATRAN could also be transformed to RGB-values – which at first glance appears to be the best possibility to compare simulations with red-green colour ratios determined from pictures. However, the transformation from the XYZ-tristimulus values to RGB-values requires additional assumptions and introduces uncertainties and is therefore not carried out in this study.

3.2 Dependence on optical depth

The left panel of Fig. 2 shows the SZA dependence of the 670 nm/550 nm radiance ratio for different values of the stratospheric AOD as grey lines. The AOD values are: 0.0, 0.05, 0.1, 0.2 and 0.3, covering the vast majority of the eruptions of the past millennium. The grey lines show simulations with constant aerosol size distribution parameters (r_{med} = 250 nm and S = 1.5),

https://doi.org/10.5194/cp-2022-38
Preprint. Discussion started: 9 May 2022
© Author(s) 2022. CC BY 4.0 License.

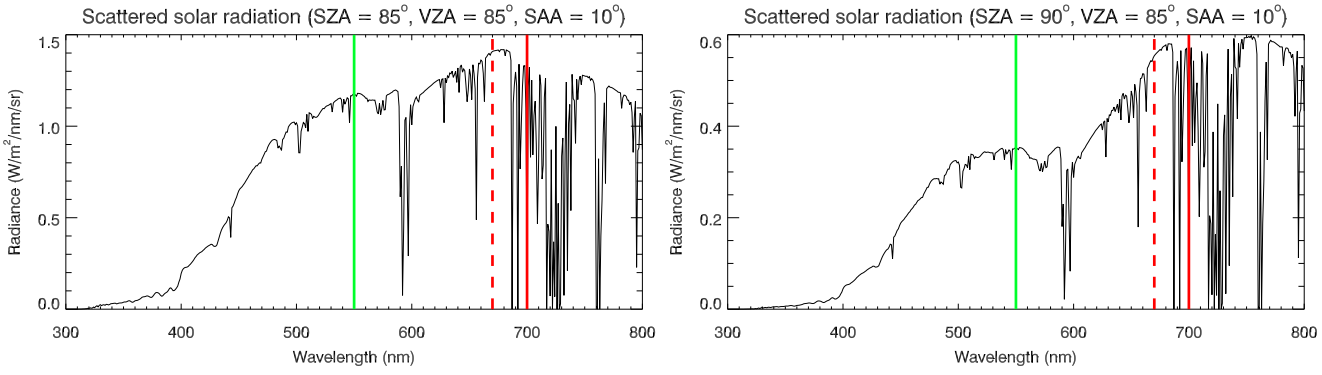

Figure 1. Sample spectra of scattered solar radiation for SZAs of 85° (left panel) and 90° (right panel) and the following parameters: VZA = 85°, SAA = 10°, TOC = 300 DU, A_S = 0.3, AOD = 0.1, r_{med} = 250 nm and S = 1.5. The green and red solid lines indicate wavelengths of 550 nm and 700 nm, while the dashed red line corresponds to 670 nm.

TOC = 300 DU, a surface albedo of 0.3 and viewing angles of VZA = 85° and SAA = 10°. Apparently and as expected, the 670 nm/550 nm radiance ratio is affected by the AOD and increases with increasing AOD value. It is interesting that the change in radiance ratio per 0.1 AOD step decreases with increasing AOD, consistent with Fig. 4 in Zerefos et al. (2007). For SZAs exceeding 90° the 670 nm/550 nm radiance ratio increases strongly with SZA and reaches values exceeding 20 at SZA = 98°. This strong SZA dependence is not observed in Fig. 4 of Zerefos et al. (2007), because their Fig. does not show the ratio of evening sky radiances, but the ratio of the diffuse downward fluxes (see also section 3.7).

The right panel of Fig. 2 shows the SZA dependence of the ratio of the tristimulus values X/Y, which is a more appropriate colour ratio to be compared to red-green-ratios extracted from historic paintings, as explained above. Qualitatively, the SZA and AOD dependence of the X/Y ratio is similar to the 670 nm to 550 nm colour ratio. However, the SZA dependence for SZA > 90° is not as strong if the ratio of the tristimulus values X and Y is used. Still, also the X/Y-ratio varies rapidly with changing SZA for SZA > 90°, rendering a quantitative determination of the AOD for SZA > 90° essentially impossible, if the actual SZA is not well known. Similar colour ratios can be produced with highly different AODs, but for different solar and viewing angles. Assuming a constant value of SZA = 100° for all paintings with SZA > 90° as in Zerefos et al. (2007) will certainly not work. Another issue related to the strong SZA-dependence of the colour ratios for SZA > 90° is the fact that evening sky colours can probably not be captured immediately in an oil painting, but the painting will take a certain time to be finished. During sunset the illumination conditions change continuously and with them also the colours of the evening sky.

3.3 Dependence on particle size

The scattering spectrum and also the colour ratios may depend sensitively on the particle size distribution of the stratospheric aerosol. In order to test this sensitivity we performed SCIATRAN simulations for different assumptions on the PSD. In all cases the PSD was assumed to be mono-modal log-normal and the geometric width was assumed to be S = 1.5. For the median radius the following values were chosen: 150 nm, 250 nm, 350 nm and 450 nm. Note that the actual PSD of stratospheric aerosols can

https://doi.org/10.5194/cp-2022-38
Preprint. Discussion started: 9 May 2022
© Author(s) 2022. CC BY 4.0 License.

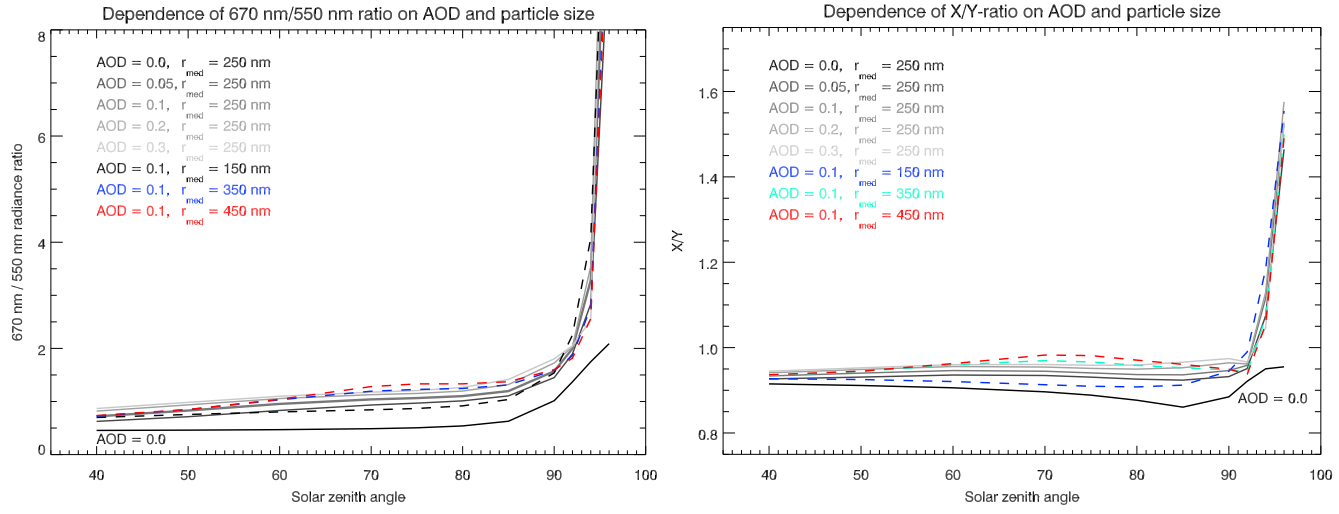

Figure 2. Ratio of the scattered solar radiances at 670 nm and 550 nm (left panel) and the X/Y tristimulus value ratio (right panel) as a function of SZA and for different values of the stratospheric AOD and different aerosol size distributions. Note that for SZAs $< 90°$ the radiance ratio increases monotonously with AOD for the AOD range shown here. Other relevant parameters: VZA = 85°, SAA = 10°, TOC = 300 DU, A_S = 0.3, S = 1.5.

be highly variable and may not always follow a mono-modal log-normal distribution (e.g. Deshler, 2008), but in many cases this assumption describes the actual PSD well. For background conditions typical values of the median radius are in the range 50 – 150 nm and for volcanically disturbed conditions, median radii exceeding 400 nm were observed, e.g. after the eruption of Mt. Pinatubo in 1991 (Bingen et al., 2004). We note that systematic differences between particle size estimates can occur if different observation geometries are used (von Savigny and Hoffmann, 2020). In addition, the variation of the stratospheric aerosol PSD after volcanic eruptions is not fully understood and a topic of current research. In a recent study, Thomason et al. (2021) showed first evidence that the mean aerosol particle size decreases after many moderate volcanic eruptions. Since the eruption of Mt. Pinatubo in 1991 led to a well observed increase in the particle size of stratospheric aerosols (e.g. Bingen et al., 2004; Deshler, 2008), it appears justified to assume an increase in particle size for strong eruptions associated with AODs exceeding ≈ 0.1, which are relevant for the present study. Note that an accurate knowledge of the PSD and its variation in the aftermath of volcanic eruptions is not crucial for the current study – we only want to test the sensitivity of the colour ratios to the PSD within a plausible range of size parameters.

The left panel of Fig. 2 shows the SZA-dependence of the 670 nm/550 nm radiance ratio for different median radii and a constant AOD of 0.1 as coloured curves. The other parameters are as listed in the Figure caption. Apparently, the effect of the particle size parameters on the colour ratios is quite large in comparison to the variations introduced by different AODs – particularly in the SZA range between 70° and 90° for which volcanic effects on the colour of the evening sky are typically observed. This implies that a determination of the AOD from colour ratios may be affected by large systematic errors if the

https://doi.org/10.5194/cp-2022-38
Preprint. Discussion started: 9 May 2022
© Author(s) 2022. CC BY 4.0 License.

Climate of the Past Discussions

actual PSD is not known. We note that Zerefos et al. (2007) do not state which PSD has been assumed for their radiative transfer simulations.

The right panel of Fig. 2 shows a similar plot but for the X/Y tristimulus value ratio. Also here the aerosol particle size distribution has a significant effect on the colour ratio, rendering a quantitative determination of the AOD essentially impossible, if no information of the aerosol PSD is available.

3.4 Dependence on ozone column

Since the overall shape of the scattering spectra can also be significantly affected by the amount of ozone in the atmosphere, we tested the impact of ozone by changing the total ozone column (TOC). For all simulations presented so far a TOC of 300 DU (Dobson Units) was assumed. Fig. 3 shows the resulting SZA-dependence of the red-green colour ratio for TOCs of 200 DU, 300 DU and 400 DU. Overall, the effect is significantly smaller than for the variable size parameters, but for SZAs between 80° and 90° an error in the assumed TOC may lead to non-negligible errors in the estimated AOD.

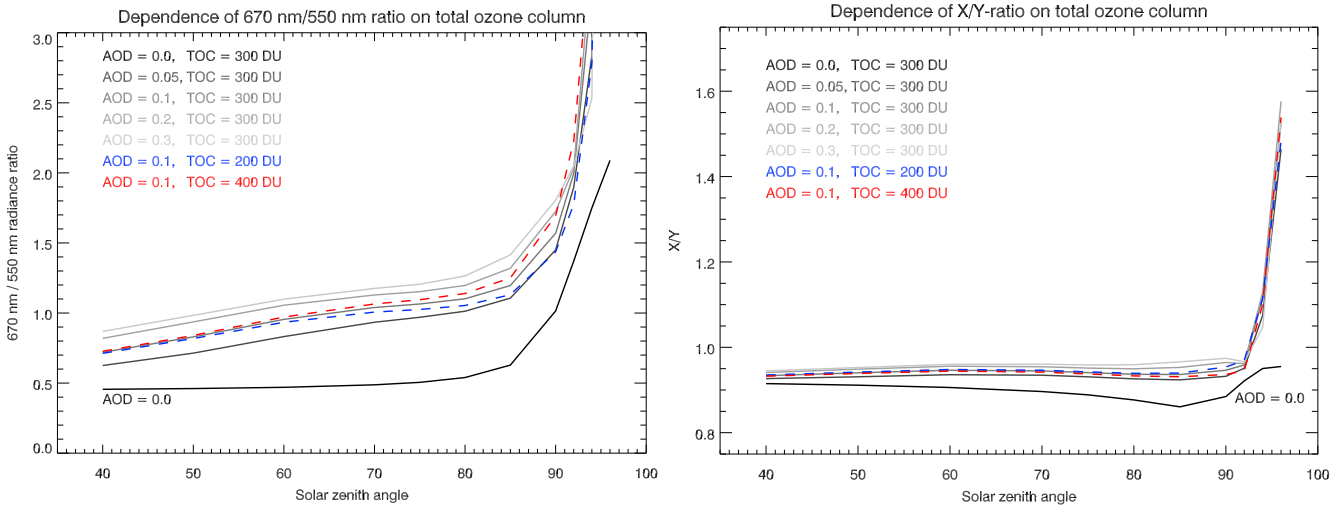

Figure 3. Ratio of the scattered solar radiances at 670 nm and 550 nm (left panel) and the X/Y tristimulus value ratio (right panel) as a function of SZA and for different values of the stratospheric AOD and TOC. Other relevant parameters: VZA = 85°, SAA = 10°, A_S = 0.3, r_{med} = 250 nm, S = 1.5.

3.5 Dependence on surface albedo

The colour ratios may also depend on the surface albedo and this impact was tested as well. Figure 4 shows a plot similar to Fig. 2 including simulation results for different values of the surface albedo. The albedo effect is relatively small, particularly for large SZAs and should only be a minor issue for the estimation of AOD from the colour ratios, also given the fact that the

https://doi.org/10.5194/cp-2022-38
Preprint. Discussion started: 9 May 2022
© Author(s) 2022. CC BY 4.0 License.

Climate of the Past Discussions

surface albedo of large fractions of the Earth is lower than about 0.3. Tropospheric clouds and tropospheric aerosols will also play a role, but they are not considered in this study.

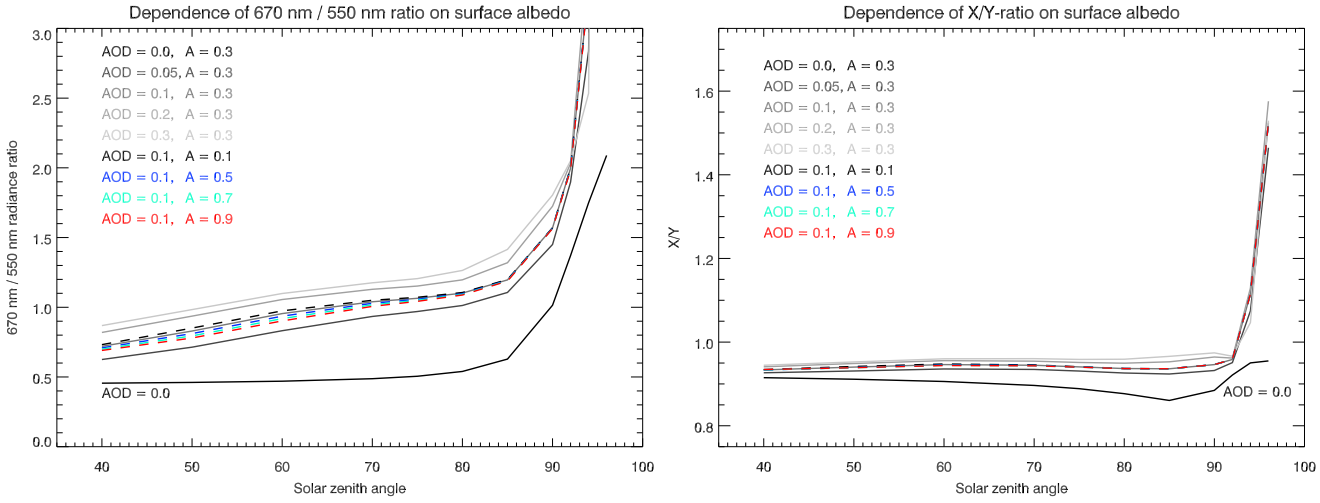

Figure 4. Ratio of the scattered solar radiances at 670 nm and 550 nm (left panel) and the X/Y tristimulus value ratio (right panel) as a function of SZA and for different values of the stratospheric AOD and different surface albedos. Other relevant parameters: VZA = 85°, SAA = 10°, TOC = 300 DU, r_{med} = 250 nm, S = 1.5.

3.6 Dependence on solar azimuth angle and viewing zenith angle

The colour ratios will certainly also depend on the specific region of the sky viewed. In order to test this effect, we performed simulations for different values of the solar azimuth angle (SAA) and the viewing zenith angle (VZA). As Fig. 5 shows, the results indicate a moderate dependence of the colour ratios on the SAA, but for viewing directions close to the horizon (VZA = 90°) a strong dependence of the colour ratios on the VZA is observed. The results imply that the actual range of viewing angles needs to be carefully considered – and the SZA needs to be precisely known, as mentioned above – when attempting to extract information on the AOD from colour ratios of the evening sky. Otherwise large systematic errors will occur. It is not explicitly mentioned in Zerefos et al. (2007), whether a specific range of viewing angles or a specific solid angle was extracted from photographs of the historic paintings. If the atmosphere close to the horizon is viewed shortly after sunset, relatively large colour ratios occur even for an aerosol-free atmosphere. This agrees with the general notion that colourful red sunsets can also occur in times without recent volcanic activity.

3.7 Relationship between diffuse downward flux and evening sky radiance

Next, we investigated the relationship between the diffuse downward flux and the evening sky radiance in order to test, whether the diffuse downward flux can be used to infer information on the aerosol optical depth, as in Zerefos et al. (2007). The left panel of Fig. 6 shows the SZA-dependence of the 670 nm/550 nm colour ratios for both the diffuse downward flux (solid lines)

https://doi.org/10.5194/cp-2022-38
Preprint. Discussion started: 9 May 2022
© Author(s) 2022. CC BY 4.0 License.

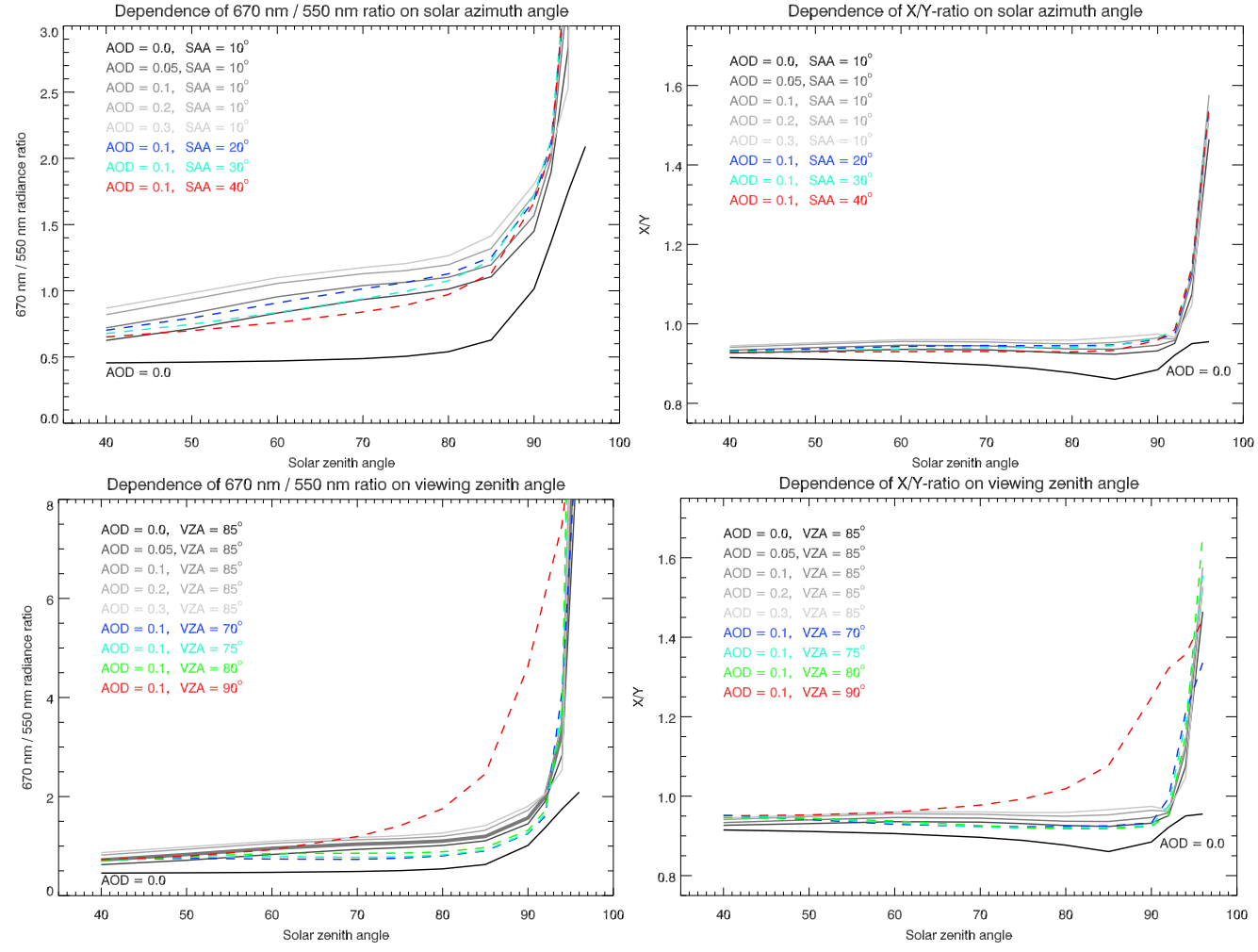

Figure 5. Ratio of the scattered solar radiances at 670 nm and 550 nm (left column) and the X/Y tristimulus value ratio (right column) as a function of SZA and for different solar azimuth angles (SAA; upper row), different viewing zenith angles (VZA; lower row) and different values of the stratospheric AOD. Other relevant parameters: TOC = 300 DU, A_S = 0.3, r_{med} = 250 nm, S = 1.5, VZA = 85° for the upper row and SAA = 10° for the lower row. Note that the ordinate ranges differ between the different panels of this Figure.

and the near-horizon radiance (dashed lines). The ratios are shown for different values of the AOD, indicated by different colours. Apparently, the radiance ratios exhibit a stronger SZA-dependence than the diffuse flux ratios. Note that the diffuse flux colour ratios exhibit a similar dependence on aerosol loading and SZA as in Fig. 3 in Zerefos et al. (2007), although the values do not match exactly. These differences could be related to the different assumptions made in Zerefos et al. (2007), e.g. the exact value of the AOD or the assumed aerosol particle size distribution. Note that the radiance ratios (as compared to the diffuse flux ratios) in the left panel of Fig. 6 are in better overall agreement with the colour ratios derived from historic paintings depicted in Fig. 3 of Zerefos et al. (2007). The results shown in the left panel of Fig. 6 already indicate that the diffuse flux

https://doi.org/10.5194/cp-2022-38
Preprint. Discussion started: 9 May 2022
© Author(s) 2022. CC BY 4.0 License.

Climate of the Past Discussions

and radiance ratios exhibit quite a different behaviour – as might be expected – which leads to non-trivial systematic errors if AOD is estimated from the diffuse flux ratio rather than the near-horizon radiance ratios. To illustrate the relationship between radiance and diffuse flux colour ratios further, the right panel of Fig. 6 shows the ratio of the radiance colour ratio and the diffuse flux colour ratio – i.e. the ratio of the dashed and solid lines in the left panel – as a function of SZA. Apparently, this ratio shows a complex dependence on SZA and AOD. The assumption of a constant scaling factor between the diffuse flux ratio and the radiance ratio can lead to large errors in the estimated AOD, if scaled simulations of the diffuse flux ratio are used to estimate AOD from the colour ratios in historic paintings, as in Zerefos et al. (2007).

We conclude that using the diffuse downward flux rather than the evening sky radiance adds additional issues that unnecessarily exacerbate the estimation of aerosol optical depth.

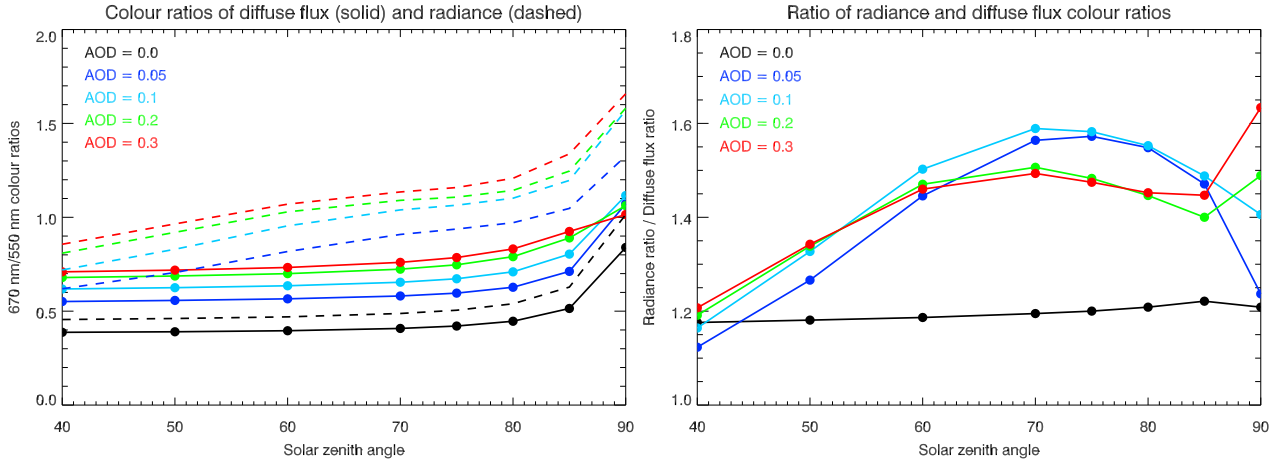

Figure 6. Left panel: SZA dependence of the 670 nm/550 nm diffuse downward flux ratio (solid lines) and radiance ratio (dashed lines) for different AOD values. Right panel: SZA dependence of the ratio between the radiance and diffuse flux ratios shown in the left panel, i.e. the ratio of the dashed and solid lines. The following parameters apply to both the diffuse flux and the radiance simulations: TOC = 300 DU, A_S = 0.3, r_{med} = 250 nm, S = 1.5 and the observer is located at the Earth's surface. The viewing angles for the radiance simulations were: VZA = 85° and SAA = 10°.

4 Discussion

We want to emphasize that we do not doubt that volcanic effects can be identified in historic paintings. Fig. 3 in Zerefos et al. (2007) demonstrates that there is a systematic difference in the red-green colour ratios between paintings in times without major volcanic eruptions and those painted in the aftermath of such eruptions. These differences are expected and are also present in the simulations shown in this study. The main aspect of this work is to show that a quantitative determination of the AOD from colours in paintings is generally not possible, if not all relevant parameters (see above) are accurately known.

https://doi.org/10.5194/cp-2022-38
Preprint. Discussion started: 9 May 2022
© Author(s) 2022. CC BY 4.0 License.

Climate of the Past Discussions

Apart from the problems described above there are several additional issues that we discuss in the following section in a qualitative way. Section 4.1 deals with the question, whether the colours in the original paintings can be expected to be realistic, using specific examples from the romanticism period. Section 4.2 addresses the issue, how colours may change due to ageing effects.

4.1 Historic Paintings as Documents? Caspar David Friedrich's intense Colours and the Beginning of Climate-Awareness

The study of Zerefos et al. (2007) assumes that paintings of the Romantic period contain precise environmental information. Historical paintings created, e.g. in the three years following the 1815 Tambora volcanic eruption are interpreted as visual archives of historic conditions of the atmosphere. However, two objections speak against this interpretation: First, the religious character of landscape in the Romantic period, and second, the difference between the event and its mediation through art. Visual representations do not speak out but speak to, i.e. paintings do not document but open up a space for interpretation as well as for reflection. Among other things, art questions our conditions of perception and our relationship to the world. Thus, although Friedrich's romantic paintings like "Greifswald in Moonshine" (1817) may be based on the experience of a particular natural event, the assumption of its documentary character drastically reduces its complexity of meaning. Realistic representations are often misinterpreted as an access to a historical reality. According to Johannes Grave, Friedrich's landscape paintings show the artist's own way of thinking about the medial conditionalities of images as well as the relationship between man and God (Grave, 2011). As a Lutheran, Friedrich shared a general scepticism towards the sense of sight, which inspired him to create a new form of religious art. His landscapes – including the painting "Greifswald in Moonshine" – are so-called composite landscapes, constructed of different locations or sketches of vegetative and geological forms (Heck, 2015). They were not painted in nature but inside of Friedrich's studio and took a certain time to be finished.

As Kilian Heck argues, a new "dialogue between viewer and image" takes place in front of Friedrich's landscapes, which leads to a conscious examination of one's relationship to nature and God (Heck, 2013). Additionally, the relatively recent ecological turn in art history has interpreted Friedrich's intense colours not as merely mirroring the artist's interest in "visual spectacles" of the atmosphere, but as negotiations of "burgeoning idea(s) about the essence of nature" (Amstutz, 2021). In an era of emerging concepts of "geological time and environmental determinism", Alexander von Humboldt, for example, valued landscape and their climates as factors influencing human physique and character alike (Amstutz, 2021). Landscape in Romanticism was also regarded as an impression of the soul. In this respect, the glow of Friedrich's colours is classified by environmental art historians as an artistic means of transgressing the material borders of the landscape paintings and creating "an environment (of reception) that had a psychological as well as a physical effect" on the viewer (Amstutz, 2021). Although, Friedrich's intense colour palette is understood as a testament to the change of the atmospheric conditions after the volcanic eruption, it is also interpreted as being part of a philosophical discussion on the moral, cultural and physical influence of nature on humankind (Amstutz and Wedekind, 2021). Therefore, Friedrich's painting "Greifswald in Moonshine" is both, an experiment of perception and a pietistic space for reflection.

https://doi.org/10.5194/cp-2022-38
Preprint. Discussion started: 9 May 2022
© Author(s) 2022. CC BY 4.0 License.


As a result, the colour intensity and luminosity in Friedrich's paintings may well be regarded by atmospheric physicists as evidence of change in the conception of nature, due to unusual light and climatic conditions following the eruption of the Tambora volcano. However, to define Friedrich's paintings, such as "Greifswald in Moonshine" as documents of a specific experience of nature or even assume a possible visualization of a quantitative determination of aerosols in the air, fails to exploit the potentials of a future cooperation between the natural sciences, arts and art history. It would be more helpful to recognise Friedrich's painting as spaces for cultural reflections on the experience, interpretation and visualisation of changing atmospheres and, on this basis, to discuss the complex relationships between incipient climate knowledge and climate awareness.

4.2 How do colours in paintings change over time?

Another potential problem is the colour change in historic paintings over time, which is an extremely complex topic. A detailed treatment is well beyond the scope of the present work and we only provide a brief discussion of some basic aspects. Among art historians and art restorers it is well accepted (e.g. Pietsch, 2014) that the ageing of a painting and the change of its colours depends on many different factors, including ratios of different pigments, the ratio of pigments and binding agents, the kind and composition of the binding agent (e.g. egg, oil, resin, glue, synthetic binder) and its specific preparation (e.g. boiled, siccativated, bleached) as well as the composition and thickness of the original and potential later coatings. In addition, the painting's individual history in terms of storage or display conditions, the light sensitivity of the individual components as well as earlier restorations need to be taken into account. In other words, the ageing and colour change would have to be investigated in detail for each individual painting and general conclusions on, e.g. the colour change per century are essentially impossible.

5 Conclusions

In this study we scrutinised the robustness of aerosol optical depth estimates from red-green colour ratios extracted from photographs of historic paintings. We emphasise that we do not challenge that colours and colour ratios in paintings of the evening sky may be affected by the stratospheric aerosol loading and volcanic effects thereon. But we question, whether quantitative information on the aerosol optical depth can be estimated. As shown by sensitivity studies using the SCIATRAN radiative transfer model, the red-green colour ratios do depend on the aerosol optical depth – as expected – but they also depend on several other factors, which are generally not known or only poorly constrained for past volcanic eruptions. We investigated the impact of the aerosol particle size distribution, total ozone column, surface albedo and the specific viewing geometry on colour ratios. The impact of surface albedo is only minor and so is the effect of the ozone column – except for large solar zenith angles. Of crucial importance is the aerosol particle size distribution, which has a strong impact on the spectral dependance of radiation scattered by the aerosols and hence on the red-green colour ratios. The effect is so large that the determination of aerosol optical depth from red-green ratios is essentially impossible for a large range of SZAs. In addition, for SZAs exceeding 90° the red-green colour ratios – irrespective of the specific wavelengths or wavelength ranges chosen – vary strongly with SZA making a quantitative estimate of the AOD very difficult, if not impossible, particularly if the actual SZA is not known.

https://doi.org/10.5194/cp-2022-38
Preprint. Discussion started: 9 May 2022
© Author(s) 2022. CC BY 4.0 License.


Also, the exact solid angle for which colour information is extracted from the photographs of paintings needs to be determined and also used for the radiative transfer simulations. Otherwise, large systematic errors have to be expected for the optical depth estimates. This effect is particularly pronounced for viewing zenith angles close to 90° and SZAs exceeding 70°. It was also found to be essential, to compare the colour ratios extracted from photographs to the correct quantity simulated with a radiative transfer model: The modelled colour ratios should be based on simulations of evening sky radiances and not on diffuse downward fluxes, as in some earlier studies. It is also questionable, whether the original colours of a painting can be considered realistic. Finally, the long-term variation of the colours in a painting would have to be carefully investigated for each individual painting and estimates of the original colours may be highly uncertain.

Code availability. The SCIATRAN radiative transfer model can be downloaded from the following website: https://www.iup.uni-bremen.de/sciatran/ (last access: April 24, 2022).

Author contributions. CvS designed the study, carried out the SCIATRAN simulations with assistance by AR and AL and wrote an initial version of the manuscript. All authors discussed and edited the manuscript. AH contributed an initial version of section 4.1.

Competing interests. The authors declare that they have no competing interests.

Acknowledgements. This work was supported by the Deutsche Forschungsgemeinschaft (project VolARC of the DFG research unit VolImpact FOR 2820, grant no. 398006378). We are indebted to the Institute of Environmental Physics of the University of Bremen – particularly to Dr. Vladimir Rozanov and Prof. Dr. John P. Burrows FRS – for providing the SCIATRAN radiative transfer model. CvS thanks Renate Kühnen and Kilian Heck (both Greifswald) for very helpful discussions.

https://doi.org/10.5194/cp-2022-38
Preprint. Discussion started: 9 May 2022
© Author(s) 2022. CC BY 4.0 License.

Climate of the Past Discussions

References

Amstutz, N.: Transparente Bilder: Caspar David Friedrichs Umgang mit Optik und Naturkunde, in: Nina Amstutz, Anne Bohnenkamp, Mareike Henning and Gregor Wedekind (ed.), Das Bild der Natur in der Romantik. Kunst als Philosophie und Wissenschaft, Paderborn, München, 119 – 145, 2021.

Amstutz, N., Wedekind, G.: Einleitung, in: Nina Amstutz, Anne Bohnenkamp, Mareike Henning and Gregor Wedekind (ed.), Das Bild der Natur in der Romantik, Kunst als Philosophie und Wissenschaft, Paderborn, München, VII-XVIII, 2021.

Bauch, M.: The Day the Sun Turned Blue: A Volcanic Eruption in the Early 1460s and Its Possible Climatic Impact – A Natural Disaster Perceived Globally in the Late Middle Ages?, in: Schenk, Gerrit J. (ed.), Historical Disaster Experiences. A Comparative and Transcultural Survey between Asia and Europe, Heidelberg, 107 – 138, 2017.

Bingen, C., Fussen, D. and Vanhellemont, F.: A global climatology of stratospheric aerosol size distribution parameters derived from SAGE II data over the period 1984–2000: 2. Reference data, J. Geophys. Res., 109, D06202, doi:10.1029/2003JD003511, 2004.

Commission Internationale De L'Eclairage (CIE): CIE 15: 2004 – Colorimetry 3rd edition, Technical Report, 2004.

Deshler, T.: A review of global stratospheric aerosol: Measurements, importance, life cycle, and local stratospheric aerosol, Atmos. Res., 90, 223–232, 2008.

Esper, J., Büntgen, U., Hartl-Meier, C., Oppenheimer, C., and Schneider, L.: Northern Hemisphere temperature anomalies during the 1450s period of ambiguous volcanic forcing, Bull Volcanol 79, 41, https://doi.org/10.1007/s00445-017-1125-9, 2017.

Grave, J.: Caspar David Friedrich: Glaubensbild und Bildkritik, Zürich, https://doi.org/10.11588/jfk.2014.1.43877, 2011.

Heck, K.: Der Betrachter ist nicht im Bilde. Ein neuer Blick auf Caspar David Friedrichs Malerei, in: Kunstchronik, 66, 365 – 355, 2013.

Heck, K.: Mimesis versus Fiktion, Präfigurationen modernen Bildverständnisses bei Caspar David Friedrich, in: Helmut Kühn und Joachum Schiedermair (ed.), Europäische Romantik: Interdisziplinäre Perpektiven der Forschung, Berlin, 65 – 82, https://doi.org/10.1515/9783110311020, 2015.

Horvath, H., Metzig, G., Preining, O., and Pueschel, R. F.: Observation of a blue sun over New Mexico, U.S.A., on 19 April 1991, Atmos. Environ., 28, 621 – 630, https://doi.org/10.1016/1352-2310(94)90039-6, 1994.

IUP, Institute of Environmental Physics/Institute of Remote Sensing (IUP/IFE), University of Bremen, Germany: User's Guide for the Software Package SCIATRAN (Radiative Transfer Model and Retrieval Algorithm) – Version 4.5, http://www.iup.uni-bremen.de/sciatran/ (last checked: April 24, 2022), 2021.

Kiessling, J.: Untersuchungen über Dämmerungserscheinungen, Voss, Hamburg und Leipzig, 1888.

Lange, A., Baumgarten, G., Rozanov, A., and von Savigny, C.: On the colour of noctilucent clouds, Ann. Geophys. Discuss. [preprint], https://doi.org/10.5194/angeo-2022-10, in review, 2022.

Laboratory for Atmospheric and Space Physics (LASP): SORCE Solar Spectral Irradiance, Spectrum. LASP Interactive Solar Irradiance Data Center (LISIRD), University of Colorado, http://lasp.colorado.edu/lisird/data/sorce_ssi_l3/, (last checked: April 24, 2022), 2003.

Pietsch, A., Material, Technik, Ästhetik und Wissenschaft der Farbe 1750 – 1850, Kunstwissenschafliche Studien, Deutscher Kunstverlag, 744 p., ISBN-13: 9783422072602, 2014.

Raible, C. C., Brönnimann, S., Auchmann, R., Brohan, P., Frölicher, T. L., Graf, H.-F., Jones, P., Luterbacher, J., Muthers, S., Neukom, R., Robock, A., Self, S., Sudrajat, A., Timmreck, C., and Wegmann, M.: Tambora 1815 as a test case for high impact volcanic eruptions: Earth system effects, WIREs Clim Change 2016, doi: 10.1002/wcc.407, 2016.

Robock, A.: Volcanic Eruptions and Climate, Rev. Geophys., 38, 191 – 219, 2000.

https://doi.org/10.5194/cp-2022-38
Preprint. Discussion started: 9 May 2022
© Author(s) 2022. CC BY 4.0 License.

Rozanov, A. V., Rozanov, V. V., Burrows, J. P.: Combined differential-integral approach for the radiation field computation in a spherical shell atmosphere: Nonlimb geometry, J. Geophys. Res., 105(D18), 22937 – 22942, 10.1029/2000JD900378, 2000.

Rozanov, V., Rozanov, A., Kokhanovsky, A., and Burrows, J.: Radiative transfer through terrestrial atmosphere and ocean: Software package SCIATRAN, J. Quant. Spec. Rad. Trans., 133, 13 – 71, 2014.

Sinnhuber, B.-M., Weber, M., Amankwah, A., and Burrows, J. P.: Total ozone during the unusual Antarctic winter of 2002, Geophys. Res. Lett., 30, 1580, doi:10.1029/2002GL016798, 2003.

Symons, G., Judd, J., Strachey, R., Wharton, W., Evans, F., Russell, F., Archibald, D., and Whipple, G.: The Eruption of Krakatoa: And Subsequent Phenomena, Krakatoa Committee of the Royal Society (Great Britain), 1888.

Thomason, L. W., Kovilakam, M., Schmidt, A., von Savigny, C., Knepp, T., and Rieger, L.: Evidence for the predictability of changes in the stratospheric aerosol size following volcanic eruptions of diverse magnitudes using space-based instruments, Atmos. Chem. Phys., 21, 1143 – 1158, doi.org/10.5194/acp-21-1143-2021, 2021.

von Savigny, C. and Hoffmann, C. G.: Issues related to the retrieval of stratospheric-aerosol particle size information based on optical measurements, Atmos. Meas. Tech., 13, 1909–1920, https://doi.org/10.5194/amt-13-1909-2020, 2020.

von Savigny, C., C. Timmreck, S. A. Buehler, J. P. Burrows, M. Giorgetta, G. Hegerl, A. Horvath, G. Hoshyaripour, C. Hoose, J. Quaas, E. Malinina, A. Rozanov, H. Schmidt, L. Thomason, M. Toohey, and B. Vogel, The Research Unit VolImpact: Revisiting the volcanic impact on atmosphere and climate - preparations for the next big volcanic eruption, Meteorologische Zeitschrift, 29, 1, 3 – 18, doi:10.1127/metz/2019/09992019, 2020.

Wullenweber, N., Lange, A., Rozanov, A., and von Savigny, C.: On the phenomenon of the blue sun, Clim. Past, 17, 969–983, https://doi.org/10.5194/cp-17-969-2021, 2021.

Zerefos, C. S., Gerogiannis, V. T., Balis, D., Zerefos, S. C., and Kazantzidis, A.: Atmospheric effects of volcanic eruptions as seen by famous artists and depicted in their paintings, Atmos. Chem. Phys., 7, 4027 -– 4042, https://doi.org/10.5194/acp-7-4027-2007, 2007.

Zerefos, C. S., Tetsis, P., Kazantzidis, A., Amiridis, V., Zerefos, S. C., Luterbacher, J., Eleftheratos, K., Gerasopoulos, E., Kazadzis, S., and Papayannis, A.: Further evidence of important environmental information content in red-to-green ratios as depicted in paintings by great masters, Atmos. Chem. Phys., 14, 2987 – 3015, https://doi.org/10.5194/acp-14-2987-2014, 2014.

Zielinski, G .A., MayewskiL, P. A., Meeker, L. D., Writlow, S. I., Twickler, M. S., Morrison, M., Meese, D. A., Gow, A. J., and Alley, R. B.: Record of volcanism since 7,000 B.C. from the GISP2 Greenland ice core and implications for the volcano-climate system, Science, 264, 948 – 952, 1994.